The Journal of Antibiotics (2010) 63, 237–243

www.nature.com/ja

ORIGINAL ARTICLE

# NBRI17671, a new antitumor compound, produced by *Acremonium* sp. CR17671

Manabu Kawada[1], Ihomi Usami[1], Tetsuya Someno[1], Takumi Watanabe[2], Hikaru Abe[2], Hiroyuki Inoue[1], Shun-ichi Ohba[1], Tohru Masuda[1], Yuji Tabata[3], Sho-ichi Yamaguchi[4] and Daishiro Ikeda[1]

**The interaction between the receptor for advanced glycation end-product (RAGE) and amphoterin has an important role in tumor growth and metastasis. Because the abrogation of the interaction results in the inhibition of the tumor growth and metastasis, we designed a screening system for an inhibitor of the interaction between RAGE and amphoterin. In the course of our screening of the inhibitor, we isolated a novel natural compound NBRI17671 (1) from the fermentation broth of *Acremonium* sp. CR17671. We also modified 1 into a more active NBRI17671al (2). Although 1 at 50 μg ml$^{-1}$ weakly inhibited binding of various cells to amphoterin, 2 at 50 μg ml$^{-1}$ inhibited it by >50% of control. Compound 2 effectively inhibited the tumor growth of glioma and lung tumor xenografts in mice at 25 mg kg$^{-1}$. Furthermore, 2 was found to downregulate mitogen-activated protein kinase (MAPK) activity in the tumor cells.**

*The Journal of Antibiotics* (2010) **63,** 237–243; doi:10.1038/ja.2010.28; published online 9 April 2010

**Keywords:** amphoterin; antitumor drug; natural compound; RAGE; tumor growth

## INTRODUCTION

The receptor for advanced glycation end-products (RAGE)[1] is a multiligand cell surface receptor and has a critical role in various diseases such as diabetes,[2] Alzheimer's disease[3] and tumor.[4] It is reported that soluble RAGE suppresses accelerated diabetic atherosclerosis by interfering the association between advanced glycation end-products and RAGE in the cells of blood vessels.[5] Because the abrogation of the association between RAGE and a respective ligand is an attractive therapeutic target, we have especially focused on tumor therapy. Amphoterin, also known as HMGB1, is one of the ligands of RAGE,[6] and is expressed at high levels in various kinds of cancers.[7] RAGE expression is not restricted to tumor cells, as cells in blood vessels also express RAGE. Thus, the interaction between RAGE and amphoterin involves not only tumor growth and motility directly, but also tumor angiogenesis.[8] Indeed, several papers reported that blockade of RAGE–amphoterin interaction suppresses tumor growth and metastasis using soluble RAGE, truncated amphoterin or antisense.[4,9,10] We therefore hypothesized that a small molecule inhibitor of the interaction between RAGE and amphoterin will become a new antitumor drug. We then designed the screening system and searched for the inhibitor. As a result, we have found a novel natural compound from a fungal strain *Acremonium* sp. CR17671. In this study we describe the isolation, structure determination and biological activity of NBRI17671 (**1**) and the synthesis and biological activity of a more active derivative of **1,** (**2**).

## RESULTS

### Isolation procedure for NBRI17671 (1)

The 5 kg culture of *Acremonium* sp. CR17671 was extracted with 10 l of 67% aqueous acetone. The filtrate of the extracts was concentrated *in vacuo* to remove acetone. The aqueous solution (3.5 l, pH 6.1) was extracted with EtOAc and the organic layer was dried over $Na_2SO_4$ and concentrated *in vacuo* to afford 11.2 g of dried materials. The materials were applied on a silica gel column (500 g, Wakogel C-200, 75–150 μm; Wako, Osaka, Japan) prepared with $CHCl_3$, and eluted with $CHCl_3$ and $CHCl_3$–MeOH. The fractions eluted with $CHCl_3$–MeOH (50:1) were concentrated *in vacuo* to give 3.0 g of crude material. The crude material was re-applied on a silica gel column prepared with $CHCl_3$–acetone (5:1) to afford 1.98 g of partially pure **1**. The sample was further applied on gel filtration chromatography of Sephadex LH-20 (GE Healthcare, Chalfont St Giles, UK) in MeOH twice to afford pure 1.94 g of **1**.

### Structure determination of NBRI17671 (1)

The physicochemical property of **1** is summarized in Table 1. Compound **1** was obtained as a white powder. This compound was readily soluble in methanol and acetone and practically insoluble in water. The molecular formula was determined to be $C_{25}H_{42}O_6$ based on the high-resolution electrospray ionization mass spectrometry, elemental analysis and NMR data. The degree of unsaturation was calculated to be five based on the molecular formula. However, the $^{13}C$ NMR

[1]Numazu Bio-Medical Research Institute, Microbial Chemistry Research Center, Shizuoka, Japan; [2]Molecular Structure Research Group, Microbial Chemistry Research Center, Tokyo, Japan; [3]Pharmaceutical Research Center, Meiji Seika Kaisha Ltd, Yokohama, Japan and [4]Bioscience Labs, Meiji Seika Kaisha Ltd, Kanagawa, Japan
Correspondence: Dr M Kawada, Numazu Bio-Medical Research Institute, Microbial Chemistry Research Center, 18-24 Miyamoto, Numazu, Shizuoka 410-0301, Japan.
E-mail: kawadam@bikaken.or.jp
Received 31 January 2010; revised 7 March 2010; accepted 8 March 2010; published online 9 April 2010

**Table 1 Physicochemical property of 1**

| | ***1*** |
|---|---|
| Appearance | White powder |
| Molecular formula | $C_{25}H_{42}O_6$ |
| Anal calcd for $C_{25}H_{42}O_6 \cdot 1/2H_2O$ | C67.08, H9.68 |
| Found | C66.63, H10.03 |
| *HRESI-MS (m/z)* | |
| Found | 461.2857 $(M+Na)^+$ |
| Calcd | 461.2879 for $C_{25}H_{42}O_6$ Na |
| UV$\lambda_{max}$ nm (MeOH) ($\varepsilon$) | 275 (10 200) |
| $[\alpha]_D^{20}$ (EtOH) | +109.6° (*c* 0.52) |

**Table 2 The $^{13}C$ and $^{1}H$ NMR assignments of 1**

| | *$CDCl_3$(40°C)* | | *Pyridine-$d_5$ (−35°C)* | |
|---|---|---|---|---|
| *Position* | *$^{13}C$ p.p.m. (mult.)* | *$^{1}H$ p.p.m. (mult., J(Hz))* | *$^{13}C$ p.p.m. (major)* | *(Minor)* |
| 1 | 193.5 (s) | | 194.0 | 194.2 |
| 2 | 145.0 (s) | | 147.8 | 146.8 |
| 3 | 140.2 (s) | | 138.5 | 142.2 |
| 4 | 55.5 (s) | | 56.0 | 54.2 |
| 5 | 41.9 (d) | 2.90 (dd, *J*=13.0, 11.0) | 41.8 | 47.5 |
| 6 | 70.7 (d) | 3.63 (dt, *J*=11.0, 3.5) | 69.8 | 70.5 |
| 7 | 36.9 (t) | 1.53 (q, *J*=11.0), 1.68 (m) | 38.5 | 37.7 |
| 8 | 34.1 (d) | 1.66 (m) | 35.3 | 35.2 |
| 9 | 67.9 (d) | 4.42 (br. s) | 67.3 | 67.3 |
| 10 | 48.0 (d) | 2.23 (dd, *J*=13.0, 2.0) | 49.4 | 49.1 |
| 11 | 35.9 (d) | 1.65 (m) | 34.8 | 33.2 |
| 12 | 33.9 (t) | 1.30 (m), 1.95 (br) | | |
| 13 | 28.5 (t) | ~1.25 (m) | | |
| 14 | 29.3[a] (t) | ~1.25 (m) | | |
| 15 | 29.6[a] (t) | ~1.25 (m) | | |
| 16 | 29.8[a] (t) | ~1.25 (m) | | |
| 17 | 31.9 (t) | ~1.25 (m) | 32.0 | 32.0 |
| 18 | 22.7 (t) | ~1.25 (m) | 22.9 | 22.9 |
| 19 | 14.1 (q) | 0.87 (t, *J*=7.0) | 14.3 | 14.3 |
| 20 | 17.5 (q) | 1.16 (d, *J*=6.5) | 17.3 | 16.8 |
| 21 | 213.1 (s) | | 211.7 | 214.6 |
| 22 | ND | 2.97 (br. m)[b], 3.83 (m)[b] | 42.9 (t) | 45.5 (t) |
| 23 | 59.1 (t) | 3.83 (m), 4.02 (m) | 58.8 | 58.1 |
| 24 | 14.6 (q) | 1.37 (br. s) | 15.3 | 15.6 |
| 25 | 17.6 (q) | 1.04 (d, *J*=6.5) | 18.4 | 18.4 |
| 2-OH | | 6.40 (s) | | |
| 6-OH | | ND | | |
| 9-OH | | ND | | |
| 23-OH | | 4.00 (br. s) | | |

Abbreviation: ND, not detected.
Chemical shifts in p.p.m. from TMS as an internal standard. The $^{13}C$ and $^{1}H$ NMR were measured at 100 and 400 MHz, respectively.
[a]Assignments may be interchanged.
[b]Major peaks in pyridine-$d_5$ at −35 °C.

spectrum (in $CDCl_3$ at 22 or 40 °C) of **1** showed 24 resolved peaks, which lacked one carbon atom. During the process of investigation, we found that a methylene signal of C-22 was not observed in the above $^{13}C$ NMR spectra. On the other hand, the signals of H-22 and C-22 were clearly visible when the NMR data were acquired in pyridine-$d_5$ at –35 °C (see Table 2). Using this condition, a partial structure (-CO-$CH_2$-$CH_2$-O-) was clearly obtained by the $^{1}H$-$^{1}H$ COSY and HMBC, as shown in Figure 1. At the same time, the possible observation of tautomeric mixture made the analysis even harder. The structure determination of **1** was first carried out using $CDCl_3$ at 40 °C. Investigation of the $^{13}C$ NMR (Table 2) revealed the presence of a double bond ($\delta_C$ 140.2 and 145.0) and two carbonyl carbons ($\delta_C$ 193.5 and 213.1), accounting for three of double bond equivalents and implying two-ring systems in **1**. The presence of a substituted decaline ring was proved by the following results. Spin networks from H-8 to $H_2$-7 through H-9, H-10, H-5 and H-6 were shown in the $^{1}H$-$^{1}H$ COSY. The correlation between methyl protons ($H_3$-25) and C-8, C-7 and C-9 in the HMBC spectrum resulted in the connectivity between C-7 and C-8 forming a six-membered ring. A hydroxyl proton at $\delta_H$ 6.4 correlated with one carbonyl carbon (C-1, $\delta_C$193.5) and two olefinic carbons (C-2, $\delta_C$ 145.0 and C-3, $\delta_C$ 140.2). Singlet methyl protons ($H_3$-24) correlated with a quaternary carbon (C-4) and an olefic carbon (C-3) and a methine proton (H-5) correlated with C-4 and C-1 in the HMBC spectrum, suggesting the presence of a substituted decaline ring. In addition, the methine proton (H-5) correlated with a carbonyl carbon (C-21) indicated that the carbonyl carbon occupied adjacent to C-4. Two methylenes ($H_2$-22 and $H_2$-23) correlated with each other in $^{1}H$-$^{1}H$ COSY and the methylene protons ($H_2$-23) correlated with C-21, suggesting the connectivity of carbonyl carbon and one of two methylenes. In addition, the chemical shift of C-23 ($\delta_C$ 59.1) was indicative of hydroxy methylene. A branched long alkyl chain was connected to C-3 carbon of decaline ring as follows. Doublet methyl protons ($H_3$-20) correlated with C-3 and C-12. In addition, $H_2$-12 correlated with $H_2$-13 in the $^{1}H$-$^{1}H$ COSY spectrum, indicating the connection of C-12 and C-13. Terminal propane moiety (C17–C19) was elucidated by the $^{1}H$-$^{1}H$ COSY and HMBC, as shown in Figure 1. Although the remaining methylenes (C-14–C-16) could not be assigned because of their almost identical chemical shifts, they should be linked with the two moieties (C-13 and C-17). Thus, the planar structure of **1** was elucidated as shown in Figure 1. The relative stereochemistry of **1** was elucidated by the analysis of coupling constants and NOESY experiments. The large coupling constants between H-5 and H-6 (*J*=11.0 Hz) and between H-5 and H-10 (*J*=13.0 Hz) indicated the 1,2-diaxial relationships of *trans*-decalin. The vicinal coupling constants between H-10 and H-9 (*J*=2.0 Hz) indicated *cis* orientation. In the NOESY, the observation of NOE between H-6 and H-8 and between H-6 and H-10 indicated 1,3-diaxial orientations. In addition, the observation of NOE between $H_3$-24 and H-10 indicated that methyl moiety of C-24 should be α-orientation. On the other hand, the lack of NOE between $H_3$-20 and $H_2$-22 indicated that methyl moiety (C-20) should be located on the opposite side of C-22. Accordingly, methyl (C-20) should be α-orientation, which is consistent with the stereochemistry proposed for the closely related compound australifungin.[11] Thus, the structure of **1** was determined as shown in Figure 2.

**Synthesis of NBRI17671al (2)**

It is reported that australifungin isolated from *Sporormiella australis* shows a highly potent antifungal activity, but australifunginol, in which the β-ketoaldehyde functional group is reduced to the alcohol in australifungin, does not.[12] Because the structure of **1** was very similar to australifunginol, we synthetically derived **1** to NBRI17671al (**2**), in which the alcohol functional group was oxidized to the β-ketoaldehyde in **1**. Selective oxidation of the primary alcohol of **1** should give **2** in a straightforward manner. After the thorough

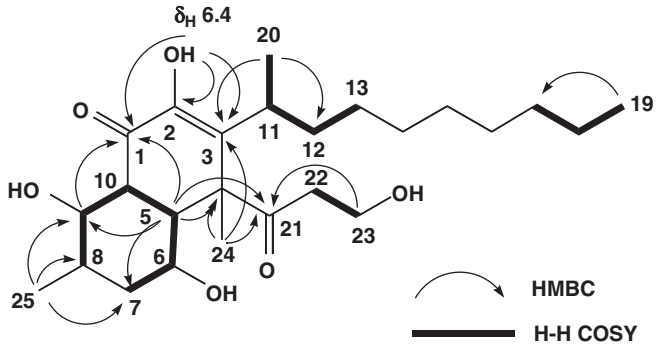


**Figure 1** $^{1}H$-$^{1}H$ COSY and HMBC of **1**.

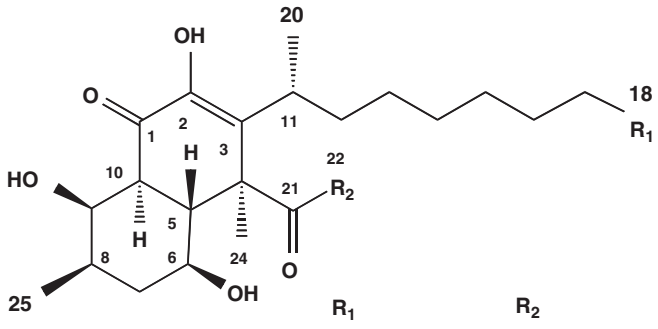


| | $R_1$ | $R_2$ |
|---|---|---|
| NBRI17671 (1) | $-CH_2CH_3$ | $-CH_2CH_2OH$ |
| NBRI17671al (2) | $-CH_2CH_3$ | -CH=CHOH |
| Australifunginol | -H | $-CH_2CH_2OH$ |
| Australifungin | -H | -CH=CHOH |

**Figure 2** Structures of **1**, **2**, australifunginol and australifungin.

screening for reaction conditions, Moffat–Pfitzner oxidation (dicyclohexylcarbodiimide, TFA and pyridine) was found to be most effective, although with moderate yield (26%). None of the secondary hydroxyl groups were affected by the method. Other conditions (tetra-*n*-propylammonium perruthenate, $SO_3$·pyridine, Dess-Martin periodinane, pyridinium chlorochromate, pyridinium dichromate, Swern oxidation, TEMPO (2,2,6,6-tetramethylpiperidine 1-oxyl) and Mukaiyama oxidation (*N*-*tert*-butylbenzenesulfenamide, *N*-chlorosuccinimide)) suffered from low conversion to end up with recovery of the substrate **1**.

### Biological activities

As shown in Figure 3a, human umbilical vein endothelial cells (HUVECs) adhered to the amphoterin-coated plates, but not to only bovine serum albumin-blocked plates without amphoterin. We applied this assay system for screening of RAGE inhibitors and found **1**. When we used RAGE-expressing cell lines such as HUVEC, A549 and 3LL cells,[4,13] **1** weakly inhibited the adhesion of these cell lines to amphoterin with $IC_{50}$'s of 82.4, 90.8 and 61.6 μg ml$^{-1}$, respectively (Figure 3b). On the contrary, **2** was expectedly found to inhibit the cell adhesion of HUVEC, A549 and 3LL cells more potently with $IC_{50}$'s of 38.0, 33.8 and 33.2 μg ml$^{-1}$, respectively (Figure 3b). As shown in Figure 3c, **1** inhibited the growth of HUVEC, A549 and 3LL cells with $IC_{50}$'s of 27.9, 70.6 and 60.5 μg ml$^{-1}$, respectively, whereas **2** inhibited them with $IC_{50}$'s of 31.9, 34.5 and 27.9 μg ml$^{-1}$, respectively.

Acute toxicity of **1** and **2** in mice was examined using ICR female mice. When **1** was administered intraperitonealy, no fatality was observed up to 100 mg kg$^{-1}$. On the other hand, mice died by intraperitoneal administration of **2** that was $>25$ mg kg$^{-1}$. We then examined the antitumor effects of both compounds against 3LL and C6 tumors in mouse models. As reported, both 3LL cells and C6 glioma cells express RAGE and amphoterin, and blockade of RAGE–amphoterin results in suppression of these tumors in mice.[4] As shown in Figure 4a, **1** failed to suppress the growth of 3LL tumors, but **2** at 25 mg kg$^{-1}$ effectively inhibited them to the same extent as adriamycin. Compound **2** also potently inhibited the growth of C6 glioma tumors in nude mice (Figure 4b).

To understand the mechanism of actions of **1** and **2** on tumor growth, we examined the effect of both compounds on the intracellular signals, because RAGE–amphoterin association triggers the activation of mitogen-activated protein kinase (MAPK).[4] As a result, compound **2**, but not **1**, significantly inhibited the activation of MAPK in 3LL cells, but both compounds did not affect Akt and IκB-α (Figure 5).

Compound **1** did not show antimicrobial and antifungal activities, but **2** showed antifungal activity especially against *Trichophyton rubrum* with MIC of 0.25 μg ml$^{-1}$.

## DISCUSSION

By screening of RAGE inhibitors among microbial cultures, we found **1** from *Acremonium* sp. CR17671. However, as the inhibitory activity of **1** against RAGE was very weak, we then tried to derive **1** to a more potent compound. It is reported that australifungin, but not australifunginol, in which β-ketoaldehyde functional group is reduced to alcohol in australifungin, inhibits sphingolipid biosynthesis and shows a highly potent antifungal activity.[12] Because the structure of **1** was very similar to australifunginol, we hypothesized that a derivative of **1**, in which the alcohol functional group was oxidized to the β-ketoaldehyde in **1**, could show more potent activity. We therefore synthetically derived **1** into **2**, and examined the effect of **2** on tumor cells. As a result, **2** expectedly showed more potent anti-RAGE and antitumor activities (Figures 3 and 4). It is interesting to note that antifungal activity was also strengthened in **2**. This result correlates well with that of australifungin,[12] suggesting that the mechanism of action of **2** against fungus will be similar to australifungin. Although the antitumor activity of australifungin is still unknown, **2** possibly inhibits the tumor growth through downregulation of MAPK (Figure 5). It is considered that the downregulation of MAPK results from the blockade of RAGE–amphoterin association by **2**.

Ohtsu *et al.*[14–16] reported that FR225654, a structurally similar compound with **2**, has a hypoglycemic effect in mouse models. We therefore tested whether **1** and **2** have such effects. As a result, both compounds could not affect glucose level in mice serum by intraperitoneal administration (data not shown). Thus, we concluded that **1** and **2** do not have a hypoglycemic effect.

## METHODS

### Cells

HUVECs were obtained from DS Pharma Biomedical (Osaka, Japan) and maintained in MCDB-131 medium (Kurorera Kogyo, Tokyo, Japan) supplemented with 10% fetal bovine serum (ICN Biomedicals, Aurora, OH, USA). Mouse Lewis lung carcinoma (3LL) cells and rat C6 glioma cells were also from DS Pharma Biomedical, and Rat1-R12 fibroblasts and human lung cancer A549 cells were from the American Type Culture Collection (Manassas, VA, USA).

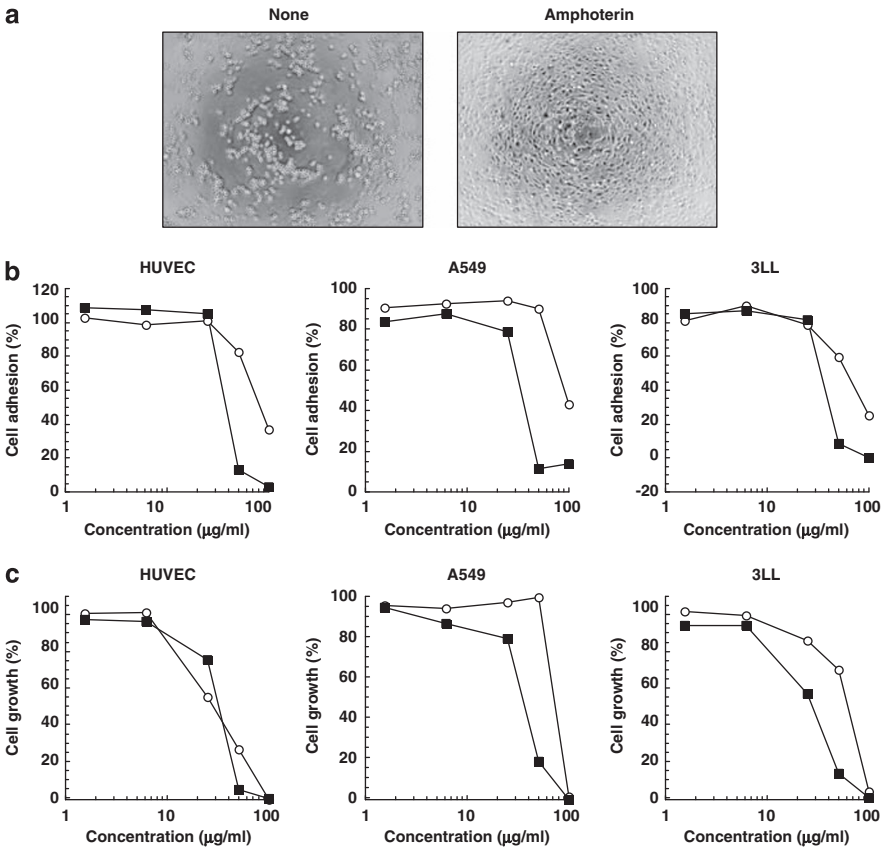


**Figure 3** Effects of **1** and **2** on cell adhesion to amphoterin-coated plates. (**a**) HUVEC was inoculated into amphoterin-coated (amphoterin) or uncoated (none) plates. (**b**) The cells were incubated in amphoterin-coated plates in the presence of the indicated concentrations of **1** (○) and **2** (■). Values are means of duplicate determinations. Each SE is <10%. (**c**) The cells were cultured for 3 days in the presence of the indicated concentrations of **1** (○) and **2** (■). The cell growth was determined using MTT. Values are means of duplicate determinations. Each SE is <10%.

They were maintained in Dulbecco's modified Eagle's medium supplemented with 10% fetal bovine serum, 100 units $ml^{-1}$ penicillin G and 100 μg $ml^{-1}$ streptomycin at 37 °C with 5% carbon dioxide.

### Preparation of recombinant amphoterin

Total RNA was extracted from Rat1-R12 fibroblasts using RNeasy Minikit (Qiagen, Hilden, Germany). The complementary DNA was synthesized using AMV reverse transcriptase (Promega, Madison, WI, USA). A *Sac*I-*Sma*I fragment of PCR-amplified rat amphoterin complementary DNA containing the full-length coding region was subcloned into pQE30 (Qiagen), yielding a construct that encodes amphoterin tagged with hexahistidine at the C-terminus. The protein was expressed in BL21 bacteria and purified using Ni-NTA resin (Qiagen) according to the manufacturer's protocol.

### Cell binding assay

First, 96-well plates were pre-incubated with the recombinant amphoterin (1.5 μg per well) in 0.05 M carbonate/bicarbonate buffer (pH 9.6) at 37 °C with 5% carbon dioxide overnight. The plates were washed twice with phosphate-buffered saline (PBS) and further incubated with 1% bovine serum albumin in PBS at room temperature for 1 h. The plates were then washed twice with PBS and used as amphoterin-coated plates. Cells ($3\times10^5$ cells per ml) in serum-free Dulbecco's modified Eagle's medium were inoculated with test samples into the amphoterin-coated plates at 100 μl per well and incubated at 37 °C with 5% carbon dioxide for 90 min. The plates were washed twice with PBS and adhered cells were fixed with 5% glutaraldehyde in PBS at room temperature for 30 min. The plates were washed with tap water and dried at 60 °C for 1 h. The cells were then stained with 0.4% crystal violet in 20% MeOH. After washing and drying the plates, the stained cells were dissolved in 1 mM HCl in 30% EtOH and absorbance at 540 nm was measured using a microplate reader.

### Cytotoxicity

Cells were inoculated in 96-well plates at 5000 cells per well with test samples and cultured for 3 days. The growth was determined using 3-(4,5-dimethylthiazol-2-yl)-2,5-diphenyltetrazolium bromide (MTT; Sigma, St Louis, MO, USA).

### Antitumor effect *in vivo*

Female C57BL/6 mice, 6 weeks old, and female nude mice, 6 weeks old, were purchased from Charles River Breeding Laboratories (Yokohama, Japan) and maintained in a specific pathogen-free barrier facility according to our institutional guidelines. 3LL cells and C6 glioma cells were trypsinized and resuspended in 10% fetal bovine serum/Dulbecco's modified Eagle's medium at $1\times10^7$ and $2\times10^7$ cells per ml, respectively. A total of 100 μl of the cell suspension of 3LL cells ($1\times10^6$ cells) and C6 glioma cells ($2\times10^6$ cells) was injected subcutaneously in the left lateral flank of C57BL/6 mice and nude mice, respectively. Five mice were used for each experimental set. Tumor volume was estimated using the following formula: tumor volume ($mm^3$)=(length×width$^2$)/2. After the indicated times, tumors were surgically dissected.

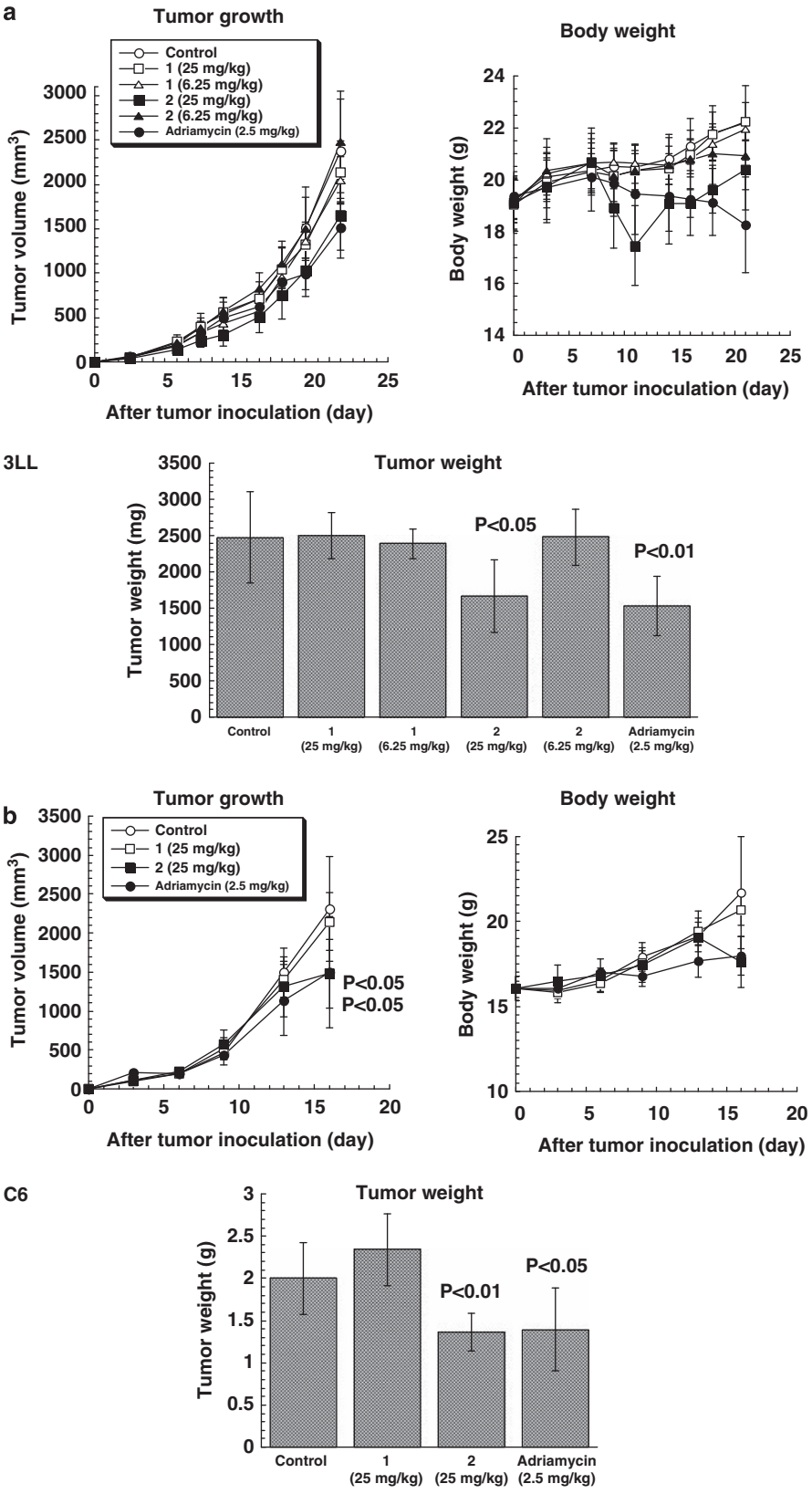


**Figure 4** Effects of **1** and **2** on tumor growth of 3LL (**a**) or C6 glioma (**b**) cells *in vivo*. 3LL and C6 glioma cells were inoculated subcutaneously in female C57BL/6 and female nude mice, respectively. Compound **1** and **2** were administered intraperitonealy on days 1–5, 7–11 and 13–19 for 3LL tumors, and days 4–7 and 11–14 for C6 glioma tumors. The values are means ± s.d. of five mice. The 3LL and C6 glioma tumors were excised at day 21 and day 16, respectively, and weighed.

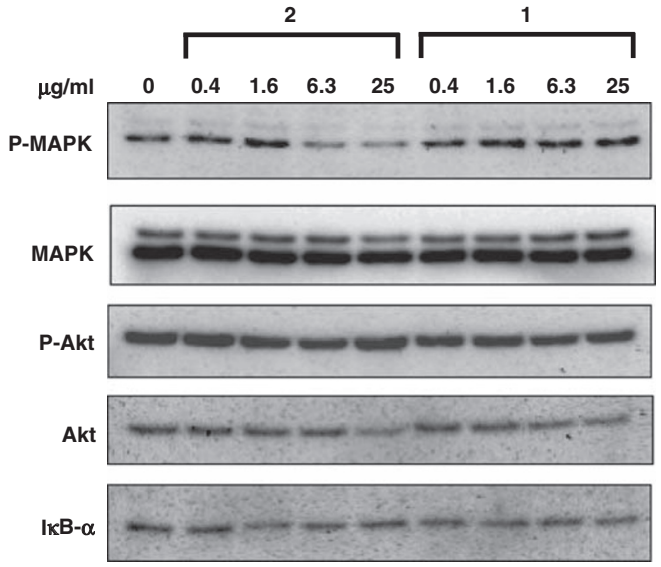


**Figure 5** Effects of **1** and **2** on intracellular signals in 3LL cells. 3LL cells were cultured with the indicated concentrations of **1** or **2** overnight. Cell lysates were prepared and western blotting was performed using the indicated antibodies.

### Preparation of cell lysates and western blotting

3LL cells ($3\times10^5$) were cultured with test samples in 10% fetal bovine serum/Dulbecco's modified Eagle's medium at 37 °C overnight. Cell lysates were prepared and applied to western blotting with antibodies as previously described.[17] Antibodies used were anti-MAPK (sc-093 and sc-154), anti-phospho-MAPK (sc-7383) and anti-IκB-α (sc-847) (Santa Cruz Biotechnology, Santa Cruz, CA, USA) and anti-Akt and anti-phospho-Akt (Thr308) (Cell Signaling Technology, Danvers, MA, USA).

### Analytical measurement

Melting points were determined with a Yanagimoto micro melting point apparatus (Yanagimoto, Kyoto, Japan) and were uncorrected. IR spectra were measured with a Horiba FT-210 spectrometer (Horiba, Kyoto, Japan). Optical rotations were measured on a JASCO P-1030 polarimeter (JASCO, Tokyo, Japan). UV spectra were recorded on a Hitachi 228 A spectrometer (Hitachi, Tokyo, Japan). $^1$H and $^{13}$C NMR spectra were measured on a JEOL JNM A400 (400 MHz) or JEOL JMN ECA 600 (600 MHz) spectrometer (JEOL, Tokyo, Japan) using TMS as an internal standard. High-resolution electrospray ionization mass spectrometry spectra were measured with a JEOL JMS-T100LC spectrometer (JEOL).

### Fermentation of fungal strain CR17671

*Acremonium* sp. CR17671 was isolated from a soil sample collected in Okayama, Japan. A slant culture of *Acremonium* sp. CR17671 was used to inoculate 100-ml Erlenmeyer flasks. Each contained 20 ml of a seed medium consisting of 2.0% soluble starch, 1.0% glucose, 0.2% soybean meal, 0.6% wheat germ, 0.5% polypeptone, 0.3% yeast extract and 0.2% $CaCO_3$ in deionized water adjusted to pH 7.2 with NaOH solution before sterilization. The flasks were incubated at 25 °C for 72 h on a rotary shaker at 220 r.p.m. Portions of 1.0 ml of this seed culture were transferred into six 500-ml Erlenmeyer flasks, each of which contained 100 ml of a seed medium. The flasks were incubated at 25 °C for 48 h on a rotary shaker at 220 r.p.m. Portions of 150 ml of this seed culture were transferred into a stainless vat containing 2.5% soybean meal and water-absorbed rice 5 kg as solid production medium. The stainless vat was thoroughly stirred and then statically cultured at 25 °C for 14 days. After incubation, 5 kg portion of the obtained culture was extracted with 10 l of 67% aqueous acetone.

### Synthesis

Dehydrated organic solvents were purchased (Kanto Chemical, Tokyo, Japan) and used without further purification. The reaction was monitored with analytical TLC using precoated silica-gel plates (Merck, Darmstadt, Germany; Silica Gel 60 $F_{254}$).

To a solution of 40.5 mg of **1** (0.0923 mmol) in 0.5 ml of toluene/DMSO (3:1) were added pyridine (7.5 ml, 92.3 mmol), TFA(6.9 ml, 92.3 mmol) and dicyclohexylcarbodiimide (28.6 mg, 0.138 mmol) successively at room temperature. The mixture was then stirred at ambient temperature for 3 h, and diluted with EtOAc followed by sequential washing with 1 M HCl, saturated $NaHCO_3$ and brine. The organic layer was dried over $Na_2SO_4$ and concentrated to dryness. The resulting residue was purified by HPLC (column: Inertsil ODS, GL Sciences, Tokyo, Japan; 20 mm×250 mm, eluent: 60–100% $CH_3CN/H_2O$ linear gradient, 0–80 min; flow rate: 8 ml min$^{-1}$) to give 10.5 mg (0.0241 mmol) of **2** in 26% yield as a yellow powder: mp 72.5–73.5 °C; $[\alpha]_D^{20}$ +119.6° (c 0.47, $CHCl_3$); IR (KBr): 2958, 1664, 1628, 1398, 1178, 1045, 987 cm$^{-1}$; $^1$H NMR (600 MHz, $CD_2Cl_2$; −40 °C) δ 9.48 (1H, d, *J*=4.1 Hz), 7.27 (1H, dd, *J*=10.3, 5.2 Hz), 5.72 (1H, d, *J*=5.5 Hz), 4.33 (1H, brs), 3.60 (1H, m), 2.59 (1H, dd, *J*=13.7, 10.3 Hz), 1.25 (3H, s), 1.06 (3H, d, *J*=6.5 Hz), 0.95 (3H, d, *J*=6.5 Hz), 0.80 (3H, t, *J*=7.0 Hz); $^{13}$C NMR (150 MHz, $CD_2Cl_2$; −40 °C) δ 207.6, 193.7, 166.5, 144.5, 139.7, 101.8, 70.2, 67.4, 53.2, 47.5, 43.9, 36.4, 34.9, 33.5, 31.9, 29.7, 29.4, 29.4, 28.0, 22.8, 17.5, 16.8, 14.1, 13.2; high-resolution electrospray ionization mass spectrometry *m/z*: calcd for $C_{25}H_{40}O_6Na$, 459.2723, found 459.2728 $(M+Na)^+$.

Compound **2** was obtained as a complex mixture of tautomers,[11] and the $^1$H and $^{13}$C NMR signals depicted above are those of the predominant enol form as shown in Figure 2.

## ACKNOWLEDGEMENTS

We are grateful to Drs S Gomi, T Kunisada and M Yonezawa (Meiji Seika Kaisha, Ltd) for their valuable discussions. We also thank Dr R Sawa and Ms Y Kubota (Microbial Chemistry Research Center) for analysis of HRESI-MS and NMR measurements. This work was supported in part by a grant-in-aid from the Ministry of Education, Culture, Sports, Science and Technology of Japan.

1 Neeper, M. *et al.* Cloning and expression of a cell surface receptor for advanced glycosylation end products of proteins. *J. Biol. Chem.* **267,** 14998–15004 (1992).
2 Yamagishi, S. *et al.* Receptor-mediated toxicity to pericytes of advanced glycosylation end products: a possible mechanism of pericyte loss in diabetic microangiopathy. *Biochem. Biophys. Res. Commun.* **213,** 681–687 (1995).
3 Yan, S. D. *et al.* RAGE and amyloid-beta peptide neurotoxicity in Alzheimer's disease. *Nature* **382,** 685–691 (1996).
4 Taguchi, A. *et al.* Blockade of RAGE-amphoterin signalling suppresses tumour growth and metastases. *Nature* **405,** 354–360 (2000).
5 Park, L. *et al.* Suppression of accelerated diabetic atherosclerosis by the soluble receptor for advanced glycation endproducts. *Nat. Med.* **4,** 1025–1031 (1998).
6 Hori, O. *et al.* The receptor for advanced glycation end products (RAGE) is a cellular binding site for amphoterin. Mediation of neurite outgrowth and co-expression of rage and amphoterin in the developing nervous system. *J. Biol. Chem.* **270,** 25752–25761 (1995).
7 Kostova, N., Zlateva, S., Ugrinova, I. & Pasheva, E. The expression of HMGB1 protein and its receptor RAGE in human malignant tumors. *Mol. Cell Biochem.* **337,** 251–258 (2010).
8 Logsdon, C. D., Fuentes, M. K., Huang, E. H. & Arumugam, T. RAGE and RAGE ligands in cancer. *Curr. Mol. Med.* **7,** 777–789 (2007).
9 Huttunen, H. J., Fages, C. & Rauvala, H. Receptor for advanced glycation end products (RAGE)-mediated neurite outgrowth and activation of NF-kappaB require the cytoplasmic domain of the receptor but different downstream signaling pathways. *J. Biol. Chem.* **274,** 19919–19924 (1999).
10 Kuniyasu, H., Chihara, Y. & Kondo, H. Differential effects between amphoterin and advanced glycation end products on colon cancer cells. *Int. J. Cancer* **104,** 722–727 (2003).
11 Hensens, O. D., Helms, G. L., Jones, E. T. T. & Harris, G. H. Structure elucidation of australifungin, a potent inhibitor of sphinganine *N*-acyltransferase in sphingolipid biosynthesis from *Sporomiella australis*. *J. Org. Chem.* **60,** 1772–1776 (1995).
12 Mandala, S. M. *et al.* The discovery of australifungin, a novel inhibitor of sphinganine *N*-acyltransferase from *Sporormiella australis*. Producing organism, fermentation, isolation, and biological activity. *J. Antibiot.* **48,** 349–356 (1995).
13 Nakano, N. *et al.* Association of advanced glycation end products with A549 cells, a human pulmonary epithelial cell line, is mediated by a receptor distinct from the scavenger receptor family and RAGE. *J. Biochem.* **139,** 821–829 (2006).

14 Ohtsu, Y., Sasamura, H., Shibata, T., Hino, M. & Nakajima, H. The novel gluconeogenesis inhibitor FR225654 that originates from *Phoma* sp. No. 00144. II. Biological activities. *J. Antibiot.* **58,** 452–455 (2005).
15 Ohtsu, Y. *et al*. The novel gluconeogenesis inhibitor FR225654 that originates from *Phoma* sp. No. 00144. I. Taxonomy, fermentation, isolation and physico-chemical properties. *J. Antibiot.* **58,** 447–451 (2005).
16 Ohtsu, Y., Yoshimura, S., Kinoshita, T., Takase, S. & Nakajima, H. The novel gluconeogenesis inhibitor FR225654 that originates from *Phoma* sp. No. 00144. III. Structure determination. *J. Antibiot.* **58,** 479–482 (2005).
17 Kawada, M., Masuda, T., Ishizuka, M. & Takeuchi, T. 15-Deoxyspergualin inhibits Akt kinase activation and phosphatidylcholine synthesis. *J. Biol. Chem.* **277,** 27765–27771 (2002).